



Fermi National Accelerator Laboratory

FERMILAB-Conf-95/103-E

DØ

Observation of the Top Quark

**Herbert Greenlee
The DØ Collaboration**

*Fermi National Accelerator Laboratory
P.O. Box 500, Batavia, Illinois 60510*

May 1995

**Presented at the 1995 Rencontre de Physique de la Vallée d'Aoste on Results and Perspectives in Particle Physics,
La Thuile, Italy, March 5-11, 1995**

Disclaimer

This report was prepared as an account of work sponsored by an agency of the United States Government. Neither the United States Government nor any agency thereof, nor any of their employees, makes any warranty, express or implied, or assumes any legal liability or responsibility for the accuracy, completeness, or usefulness of any information, apparatus, product, or process disclosed, or represents that its use would not infringe privately owned rights. Reference herein to any specific commercial product, process, or service by trade name, trademark, manufacturer, or otherwise, does not necessarily constitute or imply its endorsement, recommendation, or favoring by the United States Government or any agency thereof. The views and opinions of authors expressed herein do not necessarily state or reflect those of the United States Government or any agency thereof.

Observation of the Top Quark*

Herbert Greenlee

Fermilab

The DØ Collaboration

Abstract

The DØ collaboration reports on a search for the Standard Model top quark in $p\bar{p}$ collisions at $\sqrt{s} = 1.8$ TeV at the Fermilab Tevatron, with an integrated luminosity of approximately 50 pb^{-1} . We have searched for $t\bar{t}$ production in the dilepton and single-lepton decay channels, with and without tagging of b quark jets. We observe 17 events with an expected background of 3.8 ± 0.6 events. The probability for an upward fluctuation of the background to produce the observed signal is 2×10^{-6} (equivalent to 4.6 standard deviations). The kinematic properties of the excess events are consistent with top quark decay. We conclude that we have observed the top quark and measure its mass to be 199_{-21}^{+19} (stat.) ± 22 (syst.) GeV/ c^2 and its production cross section to be 6.4 ± 2.2 pb.

*presented at the 1995 Recontre de Physique de la Vallée d'Aoste on Results and Perspectives in Particle Physics, La Thuile, Italy, March 5–11, 1995.

1 Introduction

The Standard Model requires that the b quark have a weak isospin partner, the hitherto unobserved top quark. The search for the top quark and the measurement of its properties are important tests of the Standard Model. Certain Standard Model parameters, including m_W , m_Z , $\sin^2 \theta_W$, and Z boson decay asymmetries depend on the top quark mass, and to a lesser extent on the Higgs boson mass, through radiative corrections involving top quark loops. Precision measurements of these parameters permit an indirect measurement of the top quark mass which can be compared to that obtained by direct measurement. These precision measurements currently suggest a top quark mass in the range 150–210 GeV/c² [1].

The most sensitive searches for the Standard Model top quark have been carried out at the Fermilab Tevatron by the CDF and DØ experiments. Recent results from these experiments, based on data from the 1992–1993 Tevatron run (run Ia), include a lower limit on m_t of 131 GeV/c² by DØ [2], a 2.8σ positive result by CDF [3], and a 1.9σ positive result by DØ [4].

In this article, we assume that the top quark is pair-produced and decays 100% of the time into a W boson and a b quark. The search is divided into seven distinct channels depending on how the two W bosons decay, and on whether or not a soft muon from a b or c quark semileptonic decay is observed. The so-called dilepton channels occur when both W bosons decay leptonically ($e\mu + \text{jets}$, $ee + \text{jets}$, and $\mu\mu + \text{jets}$). The single-lepton channels occur when just one W boson decays leptonically ($e + \text{jets}$ and $\mu + \text{jets}$). The single-lepton channels are subdivided into b -tagged and untagged channels according to whether or not a muon is observed consistent with $b \rightarrow \mu + X$. The muon-tagged channels are denoted $e + \text{jets}/\mu$ and $\mu + \text{jets}/\mu$. The data set for this analysis includes data from run Ia and run Ib with an integrated luminosity of about 50pb⁻¹, with slight differences among the seven channels. The new results from CDF [5] and DØ [6] based on new data from the ongoing 1994–1995 Tevatron run (run Ib) have increased the significance of the top quark signal to $> 4\sigma$.

2 Particle Detection

The DØ detector and data collection systems are described in Ref. [7].

Muons are detected and momentum-analyzed using an iron toroid spectrometer located outside of a uranium-liquid argon calorimeter and a non-magnetic central track-

ing system inside the calorimeter. Muons are identified by their ability to penetrate the calorimeter and the spectrometer magnet yoke. Two distinct types of muons are defined. “High- p_T ” muons, which are predominantly from gauge boson decay, are required to be isolated from jet axes by distance $\Delta\mathcal{R} > 0.5$ in η - ϕ space ($\eta = \text{pseudorapidity} = \tanh^{-1}(\cos\theta)$; $\theta, \phi = \text{polar, azimuthal angle}$), and to have transverse momentum $p_T > 12 \text{ GeV}/c$. “Soft” muons, which are primarily from b, c or π/K decay, are required to be within distance $\Delta\mathcal{R} < 0.5$ of any jet axis. The minimum p_T for soft muons is $4 \text{ GeV}/c$. The maximum η for both kinds of muons is 1.7 for run Ia data and 1.0 for run Ib data. The maximum muon η is determined by the edge of the wide angle muon spectrometer. The η restriction is tightened for some run Ib data due to forward muon chamber aging.

Electrons are identified by their longitudinal and transverse shower profile in the calorimeter and are required to have a matching track in the central tracking chambers. The background from photon conversions is suppressed by an ionization (dE/dx) criterion on the chamber track. A transition radiation detector is used to confirm the identity of electrons for $|\eta| < 1$. Electrons are required to have $|\eta| < 2.5$ and transverse energy $E_T > 15 \text{ GeV}$.

Jets are reconstructed using a cone algorithm of radius $\mathcal{R} = 0.5$.

The presence of neutrinos in the final state is inferred from missing transverse energy (\cancel{E}_T). The calorimeter-only \cancel{E}_T ($\cancel{E}_T^{\text{cal}}$) is determined from energy deposition in the calorimeter for $|\eta| < 4.5$. The total \cancel{E}_T is determined by correcting $\cancel{E}_T^{\text{cal}}$ for the measured p_T of detected muons.

3 The Counting Experiment

The event selection for this analysis is chosen to give maximum expected significance for top quark masses of 180–200 GeV/c^2 , using the ISAJET event generator [8] to model the top quark signal (assuming the Standard Model top quark pair production cross section of Ref. [9]), and using our standard background estimates as described below. In this analysis, we achieve a signal-to-background ratio of 1:1 for a top quark mass of 200 GeV/c^2 . This is a better signal-to-background ratio, but with smaller acceptance, than our previously published analyses [2, 4]. The improved rejection arises primarily by requiring events to have a larger total transverse energy by means of a cut on a quantity we call H_T . H_T is defined as the scalar sum of the E_T ’s of the jets (for the single-lepton and $\mu\mu + \text{jets}$ channels, or the scalar sum of the E_T ’s of the leading electron and the jets

Table 1: Minimum kinematic requirements for the standard event selection (energy in GeV).

| Channel | High- p_T Leptons | | Jets | | Missing E_T | | Muon Tag | Topological | |
|-------------------------|---------------------|------------|------------------|-------------------|-----------------------------|----------------|------------|-------------|---------------|
| | $E_T(e)$ | $p_T(\mu)$ | N_{jet} | $E_T(\text{jet})$ | $\cancel{E}_T^{\text{cal}}$ | \cancel{E}_T | $p_T(\mu)$ | H_T | \mathcal{A} |
| $e\mu + \text{jets}$ | 15 | 12 | 2 | 15 | 20 | 10 | - | 120 | - |
| $ee + \text{jets}$ | 20 | | 2 | 15 | 25 | - | - | 120 | - |
| $\mu\mu + \text{jets}$ | | 15 | 2 | 15 | - | - | - | 100 | - |
| $e + \text{jets}$ | 20 | | 4 | 15 | 25 | - | - | 200 | 0.05 |
| $\mu + \text{jets}$ | | 15 | 4 | 15 | 20 | 20 | - | 200 | 0.05 |
| $e + \text{jets}/\mu$ | 20 | | 3 | 20 | 20 | - | 4 | 140 | - |
| $\mu + \text{jets}/\mu$ | | 15 | 3 | 20 | 20 | 20 | 4 | 140 | - |

(for the $e\mu + \text{jets}$ and $ee + \text{jets}$ channels). In addition to our “standard” event selection, we define a “loose” event selection which does not include an H_T cut. We do this as a consistency check, and to provide a less biased event sample for the top quark mass analysis.

The signature for the dilepton channels is defined as two isolated leptons, two or more jets, and large \cancel{E}_T . The signature for the single-lepton channels is defined as one isolated lepton, large \cancel{E}_T , and three or more jets (with muon tag) or four or more jets (without tag). The single-lepton signature includes either a soft muon tag or a “topological tag” based on H_T and the aplanarity of the jets \mathcal{A} . The aplanarity is proportional to the smallest eigenvalue of the momentum tensor of the jets in the laboratory and ranges from 0–0.5. “Double-tagged” events are counted only once, as part of the muon tagged channels. A summary of the kinematic cuts can be found in Table 1.

Additional special cuts are used in the $ee + \text{jets}$, $\mu\mu + \text{jets}$, and $\mu + \text{jets}/\mu$ channels to remove background from $Z + \text{jets}$. To remove $Z \rightarrow ee$ background in $ee + \text{jets}$, we require that $|m_{ee} - m_Z| > 12 \text{ GeV}/c^2$ or $\cancel{E}_T^{\text{cal}} > 40 \text{ GeV}$. Because of $D\phi$ ’s coarse muon momentum resolution, which is limited by multiple scattering to about 20%, a dimuon invariant mass cut does not effectively remove background from $Z \rightarrow \mu\mu$ with reasonable efficiency. To remove this background, we require that the event as a whole is inconsistent with the $Z + \text{jets}$ hypothesis based on a global kinematic fit (see Fig. 1). Note that although the $\mu\mu + \text{jets}$ channel does not explicitly include a \cancel{E}_T cut, it is hard for low- \cancel{E}_T events to pass the kinematic fit. The loose event selection cuts differ from those listed in Table 1 by the

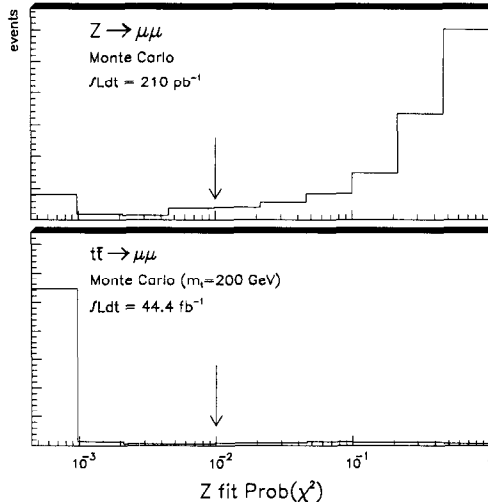


Figure 1: Chisquare probability distributions obtained from a global kinematic fit to the $Z(\rightarrow \mu\mu) + \text{jets}$ hypothesis for (a) $Z \rightarrow \mu\mu + \text{jets}$ Monte Carlo and (b) $t\bar{t} \rightarrow \mu\mu + \text{jets}$ Monte Carlo. We require $P(\chi^2) < 0.01$.

removal of the H_T requirement and by the relaxation of the aplanarity requirement for $e + \text{jets}$ and $\mu + \text{jets}$ from $\mathcal{A} > 0.05$ to $\mathcal{A} > 0.03$.

H_T is a powerful discriminator between background and high-mass top quark production. Figure 2 shows a comparison of the shapes of the H_T distributions expected from background and 200 GeV/ c^2 top quarks in the channels (a) $e\mu + \text{jets}$ and (b) untagged single-lepton + jets. We have tested our understanding of background H_T distributions by comparing data and calculated background in background-dominated channels such as electron + \cancel{E}_T + two jets and electron + \cancel{E}_T + three jets (see Fig. 3). The observed H_T distribution agrees with the background calculation, which includes contributions from both $W + \text{jets}$ as calculated by the VECBOS Monte Carlo [10] and QCD multijet events.

The acceptance for $t\bar{t}$ events is calculated using the ISAJET event generator and a detector simulation based on the GEANT program [11]. As a check, the acceptance is also calculated using the HERWIG event generator [12]. The difference between ISAJET and HERWIG is included in the systematic error.

Physics backgrounds (those having the same final state particles as the signal) are

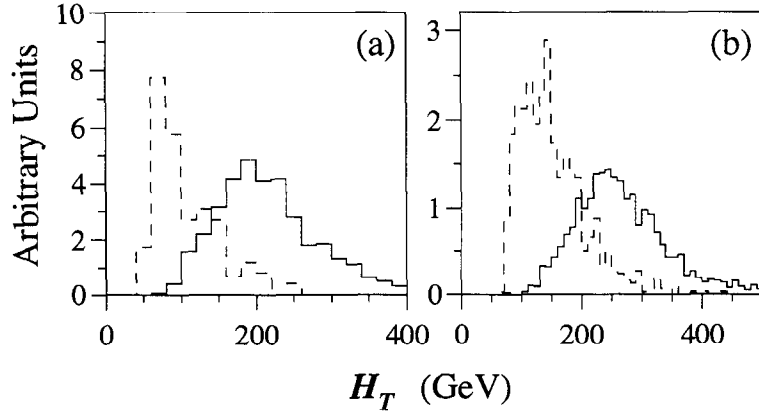


Figure 2: Shape of H_T distributions expected for the principal backgrounds (dashed line) and $200 \text{ GeV}/c^2$ top quarks (solid line) for (a) $e\mu + \text{jets}$ and (b) untagged single-lepton + jets.

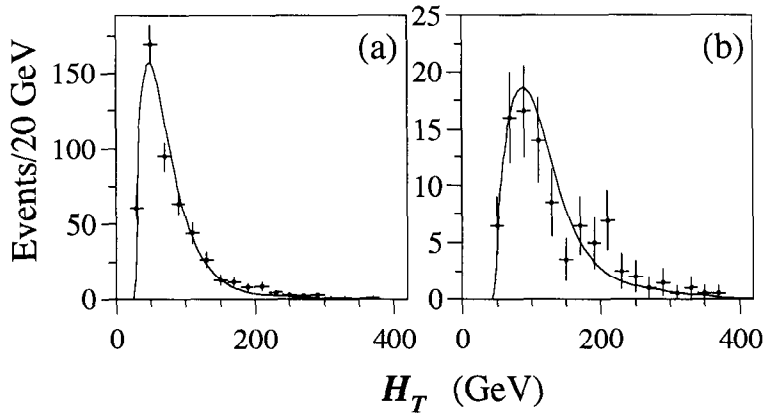


Figure 3: Observed H_T distributions (points) compared to the distributions expected from background (curve) for $\cancel{E}_T > 25 \text{ GeV}$ and (a) $e + \geq 2 \text{ jets}$ and (b) $e + \geq 3 \text{ jets}$.

estimated using Monte Carlo simulation, or a combination of Monte Carlo and data. The instrumental background from jets misidentified as electrons is estimated entirely from data using the measured jet misidentification probability (typically 2×10^{-4}). Other backgrounds for muons (*e.g.* hadronic punchthrough and cosmic rays) are negligible for the signatures in question.

For the dilepton channels, the principle backgrounds are from Z and continuum Drell-Yan production ($Z, \gamma^* \rightarrow ee, \mu\mu$, and $\tau\tau$), vector boson pairs (WW, WZ), heavy flavor ($b\bar{b}$ and $c\bar{c}$) production, and backgrounds with jets misidentified as leptons.

For the untagged single-lepton channels, the principle backgrounds are from W + jets, Z + jets, and QCD multijet production with a jet misidentified as a lepton. The W + jets background is estimated using jet-scaling. In this method, we extrapolate the W + jets cross section from one and two jets, to four or more jets assuming an exponential dependence on the number of jets, as predicted by QCD [10], and as observed experimentally (see Fig. 4). The efficiency of the topological cuts for W + 4 jets are calculated using the VECBOS Monte Carlo program [10]. The QCD multijet background is determined independently from data using the measured jet fake probability. The Z + jets background is estimated by Monte Carlo calculation.

For the tagged single-lepton channels, the observed jet multiplicity spectrum of untagged background events is convoluted with the measured tagging rate per jet to determine the total background. The tagging rate is observed to be a function of the number of jets in the event and the E_T of the jets and is the same within error for both multijet and W + jets events. As a cross check, tagging-rate predictions are made for dijet, multijet, and gamma+jet samples and found to agree with the data.

From all seven channels, we observe 17 events with an expected background of 3.8 ± 0.6 events (see Table 2). Our measured cross section as a function of the top quark mass hypothesis is shown in Fig. 6. Assuming a top quark mass of $200 \text{ GeV}/c^2$, the production cross section is $6.3 \pm 2.2 \text{ pb}$. The error in the cross section includes an overall 12% uncertainty in the luminosity. The probability of an upward fluctuation of the background to 17 or more events is 2×10^{-6} , which corresponds to 4.6 standard deviations for a Gaussian probability distribution. The excess is distributed across all of the channels in a manner consistent with Standard Model top quark decay branching ratios (see Tables 3–5). We conclude that we have observed the top quark.

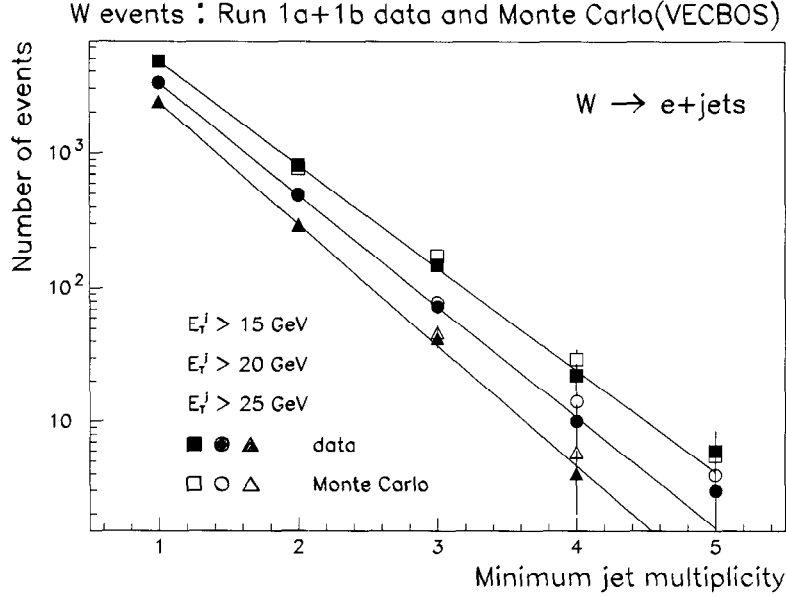


Figure 4: Inclusive jet multiplicity spectrum for $W \rightarrow e + \text{jets}$ events for several jet energy thresholds. Data are shown by the solid symbols; Monte Carlo predictions are shown by the open symbols.

Table 2: Counting experiment summary for all channels.

| | Standard Selection | Loose Selection |
|--|------------------------------------|-----------------------|
| Dileptons | 3 | 4 |
| Lepton + Jets (Topological) | 8 | 23 |
| Lepton + Jets (Muon tag) | 6 | 6 |
| All channels | 17 | 33 |
| Background | 3.8 ± 0.6 | 20.6 ± 3.2 |
| Probability | 2×10^{-6} (4.6σ) | 0.023 (2.0σ) |
| $\sigma_{t\bar{t}}$ ($m_t = 200$ GeV/ c^2) | 6.3 ± 2.2 pb | 4.5 ± 2.5 pb |

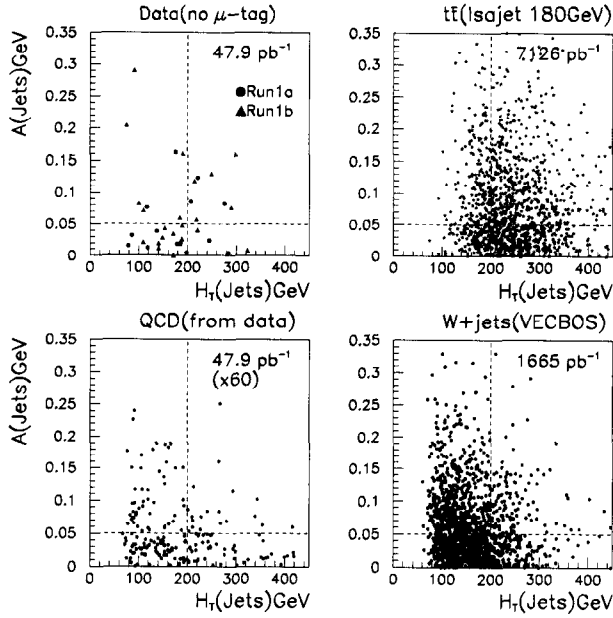


Figure 5: \mathcal{A} vs. H_T for single-lepton events for data (13.5 pb^{-1}), 180 GeV/c^2 top ISAJET Monte Carlo (7126 pb^{-1}), multijet background from data (effective luminosity = $60 \times$ data luminosity), and background from $W + 4 \text{ jet}$ VECBOS Monte Carlo (1665 pb^{-1}).

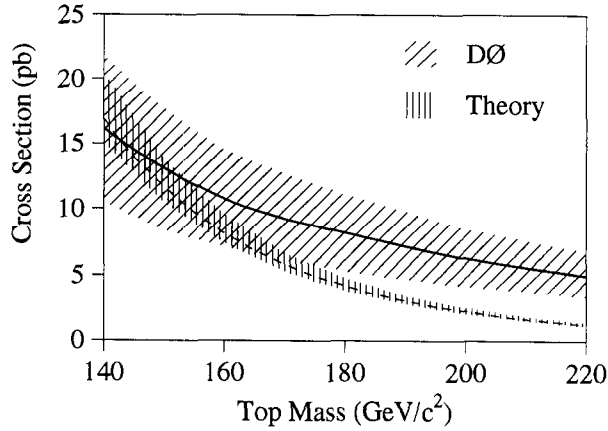


Figure 6: $D\bar{0}$ measured $t\bar{t}$ production cross section (solid line with one standard deviation error band) as a function of assumed top quark mass. Also shown is the theoretical cross section curve (dashed line) [9].

Table 3: Counting experiment summary for the dilepton channels.

| | Standard Selection | Loose Selection |
|---|--------------------------|--------------------------|
| Data | 3 | 4 |
| Background | 0.65 ± 0.15 | 2.66 ± 0.40 |
| Probability | 0.03 (1.9σ) | 0.28 (0.6σ) |
| $\sigma_{t\bar{t}}$ ($m_t = 200 \text{ GeV}/c^2$) | $7.5 \pm 5.7 \text{ pb}$ | $4.4 \pm 6.8 \text{ pb}$ |

Table 4: Counting experiment summary for the topological single-lepton channels.

| | Standard Selection | Loose Selection |
|---|--------------------------|--------------------------|
| Data | 8 | 23 |
| Background | 1.9 ± 0.5 | 15.7 ± 3.1 |
| Probability | 0.002 (2.9σ) | 0.09 (1.3σ) |
| $\sigma_{t\bar{t}}$ ($m_t = 200 \text{ GeV}/c^2$) | $4.9 \pm 2.5 \text{ pb}$ | $4.0 \pm 3.2 \text{ pb}$ |

Table 5: Counting experiment summary for the muon-tagged single-lepton channels.

| | Standard Selection | Loose Selection |
|---|--------------------------|--------------------------|
| Data | 6 | 6 |
| Background | 1.2 ± 0.2 | 2.2 ± 0.3 |
| Probability | 0.002 (2.9σ) | 0.03 (1.9σ) |
| $\sigma_{t\bar{t}}$ ($m_t = 200 \text{ GeV}/c^2$) | $8.9 \pm 4.8 \text{ pb}$ | $6.3 \pm 4.2 \text{ pb}$ |

4 Mass Analysis

We attempt to extract the top quark mass from our single-lepton + 4 jet event sample using a 2-constraint kinematic fit to the hypothesis $t\bar{t} \rightarrow W^+W^-b\bar{b} \rightarrow \ell\nu q\bar{q}b\bar{b}$. Assignment of the four highest E_T jets to partons is made using a combinatoric algorithm.

4.1 Jet Energy Corrections

We find that the chance of a successful solution of the combinatoric problem is greater using a narrower jet cone. We therefore use cone jets with radius $\mathcal{R} = 0.3$ for the mass determination as opposed to the $\mathcal{R} = 0.5$ cone jets which are used in the event selection for both the counting experiment and the mass analysis.

Correction of the measured energy inside the jet cone to the energy of the original parton takes place in two stages. The first stage, which is mainly data driven, is the correction of raw cone jets to idealized, detector-independent cone jets. The second stage, which is a theoretical construct derived from Monte Carlo studies, is the correction of the idealized cone jet to the energy of the original parton. The detector dependent corrections are for the calorimeter energy response, particle showering in and out of the cone in the calorimeter, and the subtraction of noise and energy from the underlying event.

The most important of the detector dependent corrections is the calorimeter energy response. The electromagnetic part of the energy response is fixed using resonances ($Z \rightarrow ee$, $J/\psi \rightarrow ee$, and $\pi^0 \rightarrow \gamma\gamma$). The hadronic energy scale is tied to the electromagnetic energy scale by means of E_T balance along the photon direction in “ γ ” + jet events (the photon may often be a highly electromagnetic jet). This method is a variant of the one described in Ref. [13]. The average effect of all of the detector dependent corrections is to increase the jet energy by about 20%.

The parton level energy correction is derived from the parton showering model contained in a Monte Carlo event generator, such as ISAJET or HERWIG, including the effect of a realistic detector simulation. Different corrections are used for (untagged) b quark and non- b quark jets, and for muon-tagged jets. The correction for untagged b quark and non- b -quark jets is very similar, being an upward correction of about 8% in both cases. In the case of muon-tagged jets, we include twice the momentum of the muon in the parton energy to account for the energy of the muon-neutrino.

We test our program of jet energy corrections by examining the E_T balance in $Z(\rightarrow ee) + \text{jets}$ events. We make a 1-constraint kinematic fit to the $Z + \text{jets}$ hypothesis (like

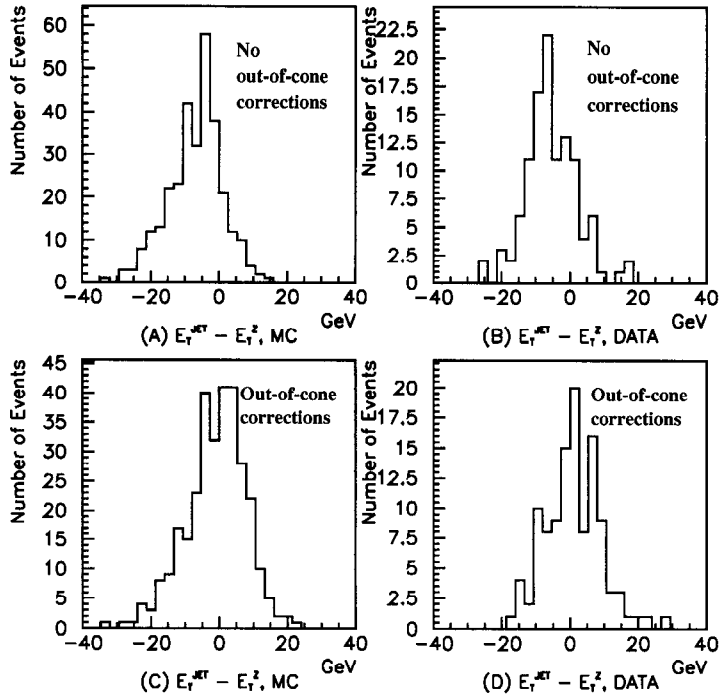


Figure 7: E_T balance in $Z + \text{jets}$ events for Monte Carlo data, with and without parton level (out-of-cone) energy corrections.

the top quark kinematic fit, but without mass constraints or jet assignment ambiguities). Figure 7 shows the E_T residuals for the jets resulting from this fit for Monte Carlo and data, with and without parton level jet energy corrections. We learn two things from this figure. First, if we compare the residuals with and without the parton energy corrections (Fig. 7(a),(b) vs. (c),(d)), we find a better accounting of the E_T balance (mean of distribution closer to zero) with parton energy corrections. Second, we see reasonable agreement between Monte Carlo and data (Fig. 7(a),(c) vs. (b),(d)) whether or not parton energy corrections are included.

4.2 Combinatoric Algorithm

In the ideal case where the four quarks give rise to four distinct jets, the number of possible solutions to the jet-parton assignment problem is twelve. In the case of a single b -tag the number of possible jet assignments is reduced to six. An additional twofold ambiguity arises from the two possible solutions for the longitudinal momentum of the neutrino

produced by the leptonically decaying W boson. Actually, the amount of ambiguity in the mass-fitting problem is larger than suggested by the above naive combinatoric analysis. Effects such as gluon radiation and jets being lost due to merging or falling below energy thresholds make the correct solution more difficult, and sometimes impossible, to find. In cases where there are more than four jets, we use only the four highest E_T jets and ignore the rest, except for their effect on the p_T of the $t\bar{t}$ system. This is equivalent to the assumption that any extra low E_T jets are due to initial state radiation. More sophisticated treatments of the fifth and higher number jets are found not to give any improvement in Monte Carlo studies.

The probability of the smallest chisquare solution being the one with the correct jet assignment is not large, being about 10–15%. It is frequently found, however, that the correct or “almost correct” jet assignments are found among the several smallest chisquare solutions. Almost correct solutions are those where the jets are assigned to the correct top quarks, but where the W boson jets are not assigned correctly. Rather than simply using the solution with the smallest chisquare, we use a chisquare-probability-weighted average top quark mass (with weight $e^{-\chi^2/2}$) from up to three solutions having $\chi^2 < 7$. It is found in Monte Carlo studies that the correct jet assignment is included in the average 25% of the time, and that an almost correct assignment is included 80% of the time. The top quark mass resolution obtained in this way is found to be slightly better than that which is obtained from the smallest chisquare solution alone (see Fig. 8).

The effects of wrong combinations, initial state gluon radiation (ISR), and final state gluon radiation (FSR), on the top quark mass resolution are shown in Fig. 9. We see from this figure that the combination of gluon radiation and combinatoric ambiguities together are much worse than either effect alone.

Despite the uncertainties and the difficulty in finding correct jet assignments, it is nevertheless found in Monte Carlo studies that the top quark mass obtained by kinematic fitting is strongly correlated with the input top quark mass. The relationship between the true (Monte Carlo) top quark mass and the mean value of the fitted top quark mass is shown in Fig. 10. The correlation is not perfect. There remains a bias that needs to be corrected when extracting the top quark mass.

4.3 Likelihood Mass Fit

An unbinned maximum likelihood fit is used to extract the top quark mass likelihood distribution from a given sample of candidate events. The likelihood function used is the

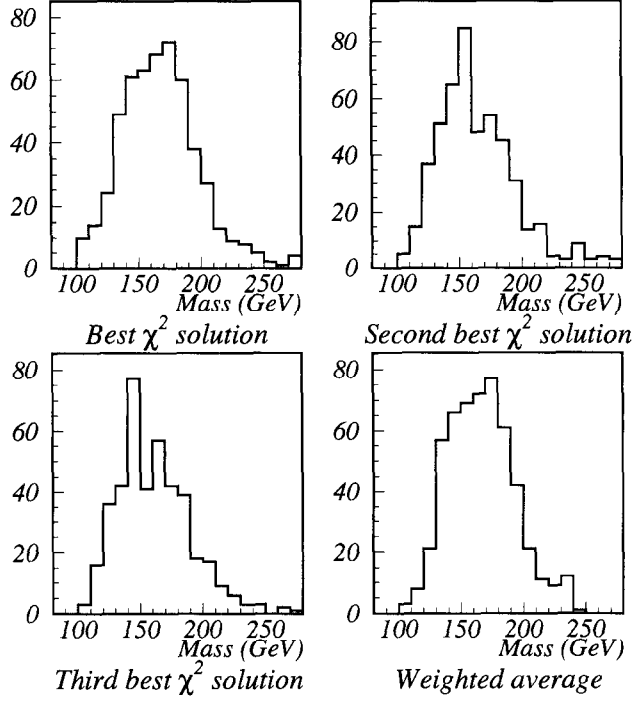


Figure 8: Top quark mass resolution obtained by averaging three best chisquare solutions for 180 GeV/c² top quark mass Monte Carlo.

following one:

$$L = e^{-(n_b - \langle n_b \rangle)^2 / 2\sigma^2} \frac{(n_s + n_b)^N}{N!} e^{-(n_s + n_b)} \prod_i \frac{n_s f_s(m_t, m_i) + n_b f_b(m_i)}{n_s + n_b} \quad (1)$$

The unknowns are the number of expected signal events n_s , the number of expected backgrounds n_b , and the top quark mass m_t . The inputs are the number of candidate events N , the fitted masses of the candidate events $m_i, (i = 1, \dots, N)$, and the nominal background $\langle n_b \rangle$ and its error σ as determined in the counting experiment. The functions f_s and f_b are the expected distributions of fitted mass for signal and background. Both f_s and f_b are determined by Monte Carlo calculation and smoothed so that they are continuous functions of m_i and m_t (f_s is shown in Fig. 11). The likelihood function consists of three multiplicative factors representing a constraint on the background normalization, overall Poisson counting statistics, and the relative likelihood for each event to be a top quark event (for a given top quark mass) or background.

The entire mass determination machinery has been tested using Monte Carlo data. We have verified that mass bias of the kinematic fit is removed by the likelihood fit, and

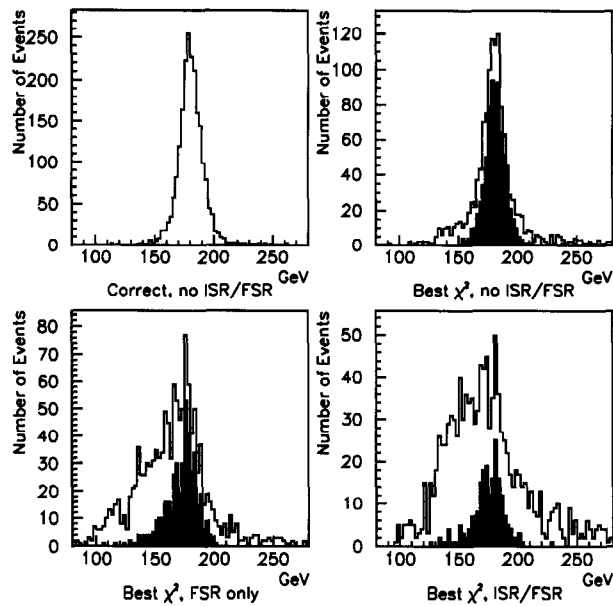


Figure 9: Effect of wrong combinations, initial and final state gluon radiation on top quark mass resolution for 180 GeV/c² top quark mass ISAJET Monte Carlo. The shaded areas of the histograms are what is obtained when Monte Carlo information is used to make the correct jet assignments in the presence of gluon radiation.

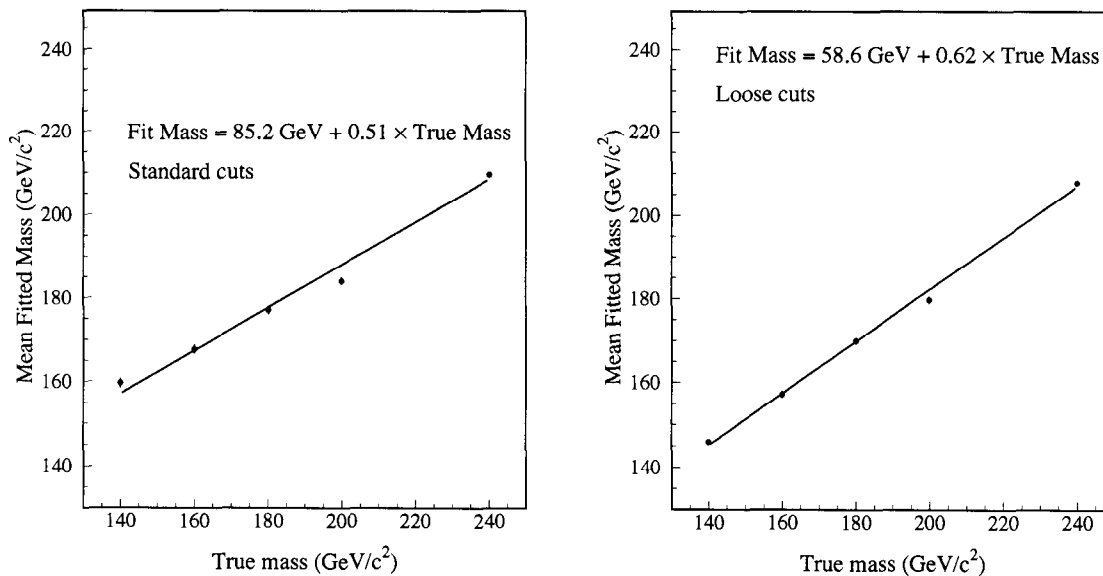


Figure 10: Fitted top quark mass vs. ISAJET input top quark mass for standard and loose selection criteria.

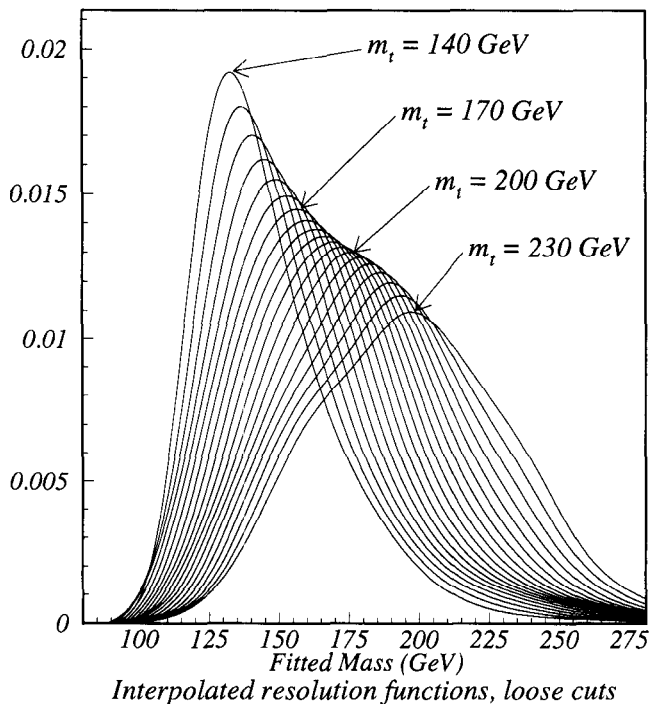


Figure 11: Smoothed and interpolated top quark mass resolution functions for the loose cuts event selection.

that the statistical error of the top quark mass from the likelihood fit scales inversely as the square root of the number of candidate events.

Eleven of the 14 single-lepton + 4 jet candidate events selected using the standard cuts, and 24 of the 27 candidate events selected using the loose cuts, have successful kinematic fits. The fitted mass and likelihood distributions of these events are shown in Fig. 12. The top quark mass extracted from the likelihood curve is 199^{+31}_{-25} (stat.) GeV/c^2 for standard cuts and 199^{+19}_{-21} (stat.) GeV/c^2 for loose cuts. The errors are statistical (so far) and are derived using $\Delta L = 0.5$. The result of the likelihood fit for the loose cuts sample does not change significantly if the background constraint is removed from the likelihood function. Because of its smaller error, we use the loose cuts mass determination as our official mass result.

The most important systematic error in the top quark mass determination is the jet energy scale uncertainty. We estimate this uncertainty to be 10% or less. We determine the error in the top quark mass by varying jet energies by $\pm 10\%$ and observing the effect on the top mass. The W mass constraint tends to compensate for energy scale errors, but

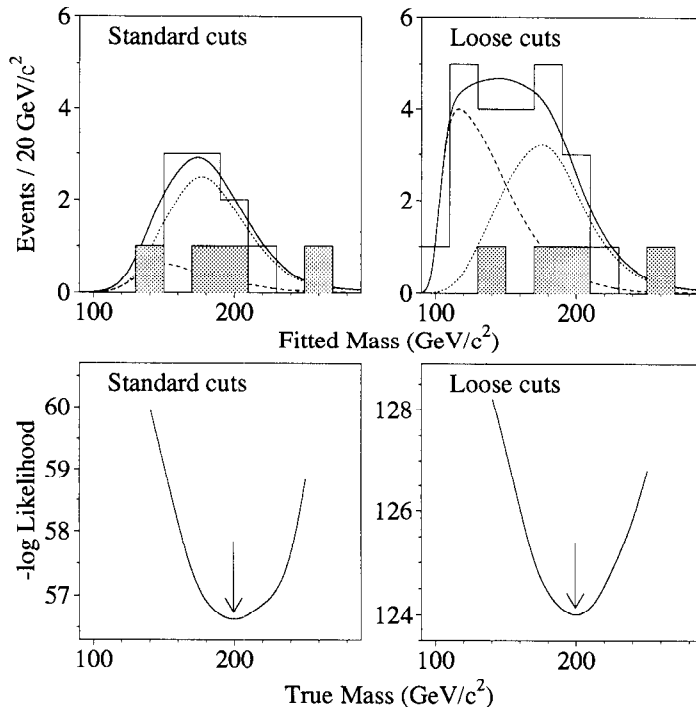


Figure 12: Fitted mass and mass likelihood distributions for standard and loose cuts. Shaded events have a soft muon tag.

the bias in the fitted mass (Fig. 10) exacerbates the energy scale error. These two effects approximately cancel, giving an 11% systematic error in the top quark mass.

The top mass measurement depends on having an event generator that realistically models effects such as gluon radiation and jet shapes. We estimate this uncertainty by comparing results obtained using ISAJET and HERWIG. Our main result is based on ISAJET. If we do all of the steps using HERWIG instead, the result is that the top quark mass is lowered by $4 \text{ GeV}/c^2$. We include this difference in the systematic error for the top quark mass, but it has little additional effect when added in quadrature with the jet energy scale error. The total systematic error on the top quark mass is $22 \text{ GeV}/c^2$.

5 Conclusions

We have searched for top quark signals in seven channels in a data sample having an integrated luminosity of 50 pb^{-1} . We observe 17 candidate events with an expected

background of 3.8 ± 0.6 events. The excess is statistically significant. The probability for the background to fluctuate up to 17 events is 2×10^{-6} , which corresponds to 4.6σ in the case of Gaussian errors. We measure the top quark mass to be $199_{-21}^{+19}(\text{stat.}) \pm 22(\text{syst.})\text{GeV}/c^2$. Using the acceptance calculated at our central top quark mass, we measure the top quark pair production cross section to be $\sigma_{t\bar{t}} = 6.4 \pm 2.2$ pb.

References

- [1] D. Schaile, CERN-PPE/94-162, presented at 27th International Conference on High Energy Physics, Glasgow, July 1994 (unpublished).
- [2] DØ Collaboration, S. Abachi *et al.*, Phys. Rev. Lett. **72**, 2138 (1994).
- [3] CDF Collaboration, F. Abe *et al.*, Phys. Rev. D **50**, 2966 (1994); Phys. Rev. Lett. **73**, 225 (1994).
- [4] DØ Collaboration, S. Abachi *et al.*, Phys. Rev. Lett. **74**, 2422 (1995).
- [5] D. Gerdes, these proceedings;
CDF Collaboration, F. Abe *et al.*, Phys. Rev. Lett. **74**, 2626 (1995).
- [6] DØ Collaboration, S. Abachi *et al.*, Phys. Rev. Lett. **74**, 2632 (1995).
- [7] DØ Collaboration, S. Abachi *et al.*, Nucl. Instrum. Methods **A338**, 185 (1994).
- [8] F. Paige and S. Protopopescu, BNL Report no. BNL38034, 1986 (unpublished), release v6.49.
- [9] E. Laenen, J. Smith, and W. van Neerven, Phys. Lett. **321B**, 254 (1994).
- [10] F. A. Berends, H. Kuijf, B. Tausk, and W. T. Giele, Nucl. Phys. B357, 32 (1991).
- [11] F. Carminati *et al.*, "GEANT Users Guide," CERN Program Library, 1991 (unpublished).
- [12] G. Marchesini *et al.*, Comput. Phys. Commun. **67**, 465, (1992).
- [13] CDF Collaboration, F. Abe *et al.*, Phys. Rev. Lett. **69**, 2898, (1992).